Reactive Collisions of H_3O^+ and OH^- Studied with the Polarization Model

Thomas A. Weber and Frank H. Stillinger*

Bell Laboratories, Murray Hill, New Jersey 07974 (Received: November 6, 1981)

Classical equations of motion have been numerically integrated for reactive collisions between hydronium and hydroxide ions. The polarization model was employed to represent the multidimensional potential energy surface for all configurations of the six nuclei encountered. Initial conditions corresponded to zero incident energy and unexcited reactants. Energy released by the neutralization reaction tends preferentially to accumulate on the neutral product molecule whose oxygen originated with the hydroxide anion. An anomalous class of "rebound" collisions was discovered wherein near symmetry of the collision complex prevents proton transfer.

I. Introduction

In order to pursue quantitative studies of molecular collision dynamics and of condensed phase structure and kinetics it is necessary to have a compact representation for the molecular interactions involved. The polarization model has been introduced for this purpose primarily to investigate the behavior of hydrogen-bonding substances.[1-6] This model spontaneously yields correct molecular structures, allows vibrations to occur, leads to realistic dielectric response, and permits molecular dissociation into ionic fragments. The chemically most significant aspect of this last feature is that it makes feasible the examination of proton solvation and transfer processes in both gas phase and in liquid solution.

Although the polarization model incorporates many-body forces, the equations describing its classical dynamics for atomic motions have forms convenient for application.[7] Indeed some aspects of the collision dynamics involving bare protons and water octamers have already been reported.[8]

This paper is devoted to a study of the elementary gas-phase neutralization reaction

$$H_3O^+ + OH^- \rightarrow 2H_2O \qquad (1)$$

Once again the polarization model has been utilized to supply a global description of the total potential energy hypersurface which is now essentially 12-dimensional (after removing translational and rotational invariances). For simplicity we have restricted attention to the dynamical case corresponding to reactants devoid of translational, rotational, or vibrational excitation when they were infinitely far apart in the remote past.

Section II presents reactant structures, energies, and specific initial conditions employed for generation of our small ensemble of trajectories. Details of the observed kinetics and of the product distributions are then given in section III. Our conclusions appear in section IV.

II. Reactant Specification

In its application to water the polarization model treats the hydrogen atoms as bare protons (charge $+e$), and the oxygen atoms as doubly charged anions (charge $-2e$). The former are unpolarizable, while the latter are assigned isotropic polarizability 1.444 $Å^3$. In an arbitrary configuration of hydrogens and oxygens the potential energy Φ is calculated in two parts[1]

$$\Phi = \Phi_{pair} + \Phi_{pol} \qquad (2)$$

The first part comprises additive central interactions between all pairs of particles present, and includes Coulombic, covalency, and overlap repulsion interactions. The second part is patterned after (but generalizes) the charge-induced dipole interactions familiar in classical electrostatics. The overall formats for Φ_{pair} and Φ_{pol} are explained in detail in ref 1, while the specific input functions employed for the present dynamical study have been collected in the Appendix.

For an isolated group of two hydrogens and one oxygen the single minimum created by the polarization model potential corresponds exactly to the nonlinear water molecule. The bond lengths are 0.9854 Å, and their angle is 104.45°. Furthermore, the net dipole moment in this configuration is 1.855 D, equal by construction to the measured value for the water molecule.[1]

The bond length implied by the function set given in the Appendix for the hydroxide anion is 0.8601 Å, somewhat shorter than that suggested by high accuracy quantum mechanical calculations (0.963 Å).[9] This imprecision is a typical price that must be paid to achieve a simple representation of the complicated general potential Φ.

The hydronium ion H_3O^+ has the requisite threefold symmetry and pyramidal shape in the present version of the polarization model. Its OH bonds are 1.036 Å long,

(1) F. H. Stillinger and C. W. David, *J. Chem. Phys.*, **69**, 1473 (1978).
(2) F. H. Stillinger, *Int. J. Quantum Chem.*, **14**, 649 (1978).
(3) C. W. David, *Chem. Phys.*, **40**, 229 (1979).
(4) F. H. Stillinger and C. W. David, *J. Chem. Phys.*, **73**, 3384 (1980).
(5) C. W. David, *Chem. Phys.*, **53**, 105 (1980).
(6) P. J. Turner and C. W. David, *J. Chem. Phys.*, **74**, 512 (1981).
(7) F. H. Stillinger, *J. Chem. Phys.*, **71**, 1647 (1979).
(8) F. H. Stillinger and T. A. Weber, *Chem. Phys. Lett.*, **79**, 259 (1981).

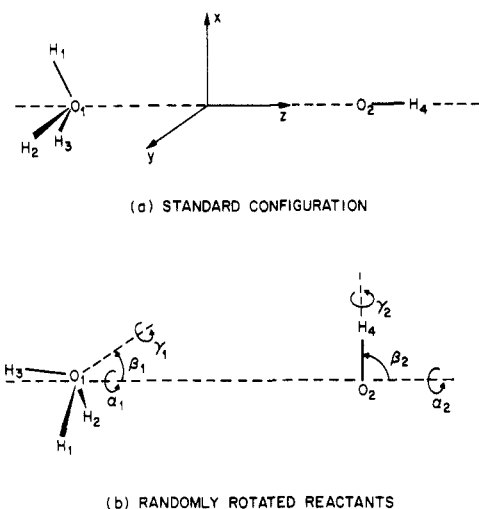(9) R. Janoschek, H. Preuss, and G. Diercksen, *Int. J. Quantum Chem.*, **1**, 649 (1967).

(a) STANDARD CONFIGURATION

(b) RANDOMLY ROTATED REACTANTS

Figure 1. Generation of initial configurations. The hydronium and hydroxide ions are first placed in the standard configuration (a) with their centers of mass 20 Å apart, and the system center of mass at the origin. Random rotations are then applied to each ion about its center of mass (b).

and lie 71.8° off the symmetry axis. The proton affinity of water, i.e., the difference in Φ for H_2O and H_3O^+ each at their respective minima, is found to be

$$\Phi[H_2O] - \Phi[H_3O^+] = 171.362 \text{ kcal/mol} \qquad (3)$$

The hydronium ion inversion barrier is predicted to be 2.039 kcal/mol. These values may be compared with those found by Diercksen, Kraemer, and Roos[10] in a quantum-mechanical study, namely 0.972 Å bond length, 72.8° apex angle, 172.8 kcal/mol proton affinity, and 2.05 kcal/mol inversion barrier.

Figure 1 indicates how the H_3O^+ and OH^- reactants are positioned at the beginning of the generation of each dynamical trajectory. The centers of mass of these two clusters are placed along the z axis of a Cartesian coordinate system, 20 Å apart, with the overall system center of mass at the origin. Each has the internal geometry corresponding to its own mechanical equilibrium. Starting from a standard orientation for the reactants, Figure 1a, random rotations are then applied to each about its own center of mass (Euler angles α_1, β_1, γ_1 for H_3O^+; α_2, β_2, γ_2 for OH^-).

Next, the change in potential energy is computed for the generated initial configuration, compared to infinitely separated reactants

$$\Delta\Phi = \Phi[H_4O_2, 20 \text{ Å}] - \Phi[OH^-] - \Phi[H_3O^+] \qquad (4)$$

This difference is invariably negative owing to the opposite charges on the reactants, although it varies with rotation angles. Since our interest is confined to simulating collisions with vanishing kinetic energy at infinite separation for reactants, $\Delta\Phi$ is used to assign initial velocities v_1 and v_2 to H_3O^+ and OH^-, respectively. These velocities are in the positive z direction for v_1, and in the negative direction for v_2, and are required to satisfy the conditions

$$M_1 v_1 + M_2 v_2 = 0$$

$$\Delta\Phi + \tfrac{1}{2}M_1 v_1^2 + \tfrac{1}{2}M_2 v_2^2 = 0 \qquad (5)$$

The hydronium mass has been denoted here by M_1, that of the hydroxide by M_2. The first of these conditions keeps the system center of mass fixed at the origin, while the

second converts $\Delta\Phi$ to kinetic energy as required.

At the beginning of each computed trajectory the ratio of hydroxide to hydronium speeds is $M_1/M_2 = 19/17$. The corresponding kinetic energy ratio is also $19/17$. The subsequent dynamical evolution has been determined by numerical solution of Newton's equations for the six particles as described below; we feel justified in using classical rather than quantum mechanics because of the large energies involved in the collision and reaction.

III. Reaction Dynamics

Dynamical trajectories have been constructed for 100 starting configurations that uniformly sample relative orientations of the reactants. Each of these trajectories was followed for 2 ps using a fifth-order Gear algorithm[11] with time increment

$$\Delta t = 6.25 \times 10^{-5} \text{ ps} \qquad (6)$$

This small increment suffices to conserve energy to reasonable accuracy during reactive collision; it cannot be chosen substantially larger owing to rapidity of proton vibrational motions, particularly during and after the collision.

With the initial conditions used it is typically the case that the charged reactants fall inward and collide after only 0.3–0.4 ps. With one exception noted below (trajectory no. 47) the excess proton on the hydronium immediately transfers to the hydroxide, and the resulting two neutral water molecules recede rapidly from one another, carrying away the considerable energy of reaction

$$\Phi[H_3O^+] + \Phi[OH^-] - 2\Phi[H_2O] = 217.506 \text{ kcal/mol} \qquad (7)$$

A major objective of this study is prediction of the way that this available energy partitions among translational, rotational, and vibrational motions.

The energy shown in eq 7 exceeds that necessary to split a water molecule into neutral H and OH radicals (about 126 kcal/mol). By its nature the polarization model is prevented from entering such a channel. But we believe that this kind of process is unlikely anyway for the conditions investigated here, since our results show that it is very improbable to concentrate enough vibrational energy in either H_2O product to effect the bond breakage.

A convenient way to follow the course of any trajectory is by plotting against time the root-mean-square distance S_0 of the oxygens from the system center of mass. Figure 2 shows such a plot for one of the "typical" reactive collisions. The initial portion of the curve has downward curvature due to the accelerations experienced by the mutually attracting reactant ions. After passing through the minimum separation (approximately 2 Å between the oxygens) the curve rises rapidly and almost linearly because the product molecules are neutral. Normally the diverging water molecules are sufficiently well separated by the time 1 ps has elapsed that we can then regard the system as having entered the asymptotic regime. Consequently the time interval between 1 ps and 2 ps has been used to calculate product distributions.

Figure 3 displays S_0 vs. t for the anomalous trajectory no. 47. It shows *two* minima, one at the expected collision time, and another at approximately 1.2 ps. The plot has downward curvature between these minima, indicative of still-ionic fragments. Evidently proton transfer failed to occur at first collision, which was followed by nonescaping rebound and then a reactive second collision. Obviously

(10) G. H. F. Diercksen, W. P. Kraemer, and B. O. Roos, *Theor. Chim. Acta* (Berlin), **36**, 249 (1975).

(11) C. W. Gear, "The Numerical Integration of Ordinary Differential Equations of Various Orders", Argonne National Laboratory Report ANL-7126, Jan 1966.
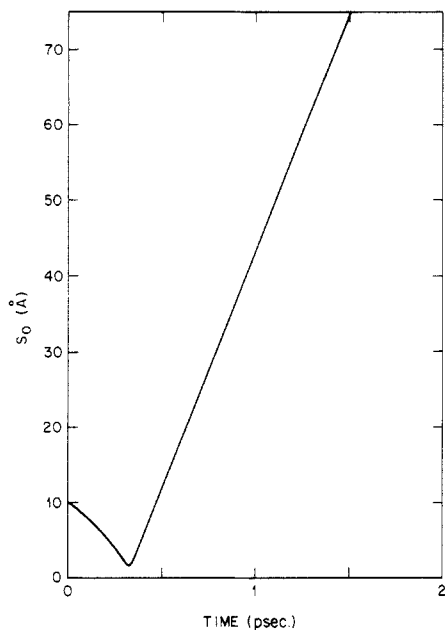
Figure 2. Root-mean-square distance of oxygens from the system center of mass vs. time. The curve shown was taken from trajectory no. 1, a typical reactive collision.
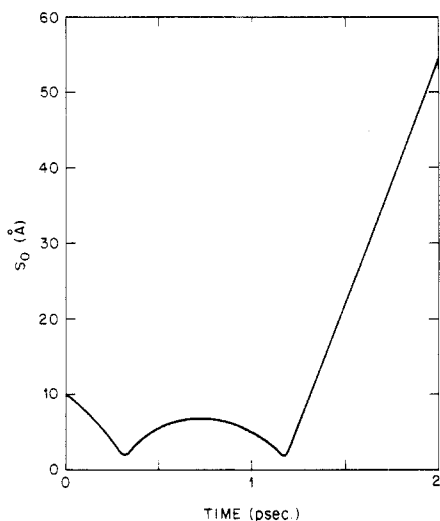

Figure 3. Root-mean-square distance of oxygens from the system center of mass for the anomalous trajectory no. 47.

this trajectory had *not* entered its asymptotic regime at 1 ps. For that reason this one case was exempted from our statistical analysis, which therefore considers averages over the remaining 99 "typical" encounters.

A little thought reveals how anomalous trajectories can occur. Only one proton has to be transferred for neutralization, but three are available on the hydronium cation. If the reactants collide in an arrangement which places the hydroxide more or less symmetrically between two of the hydronium protons, transfer of just one proton is inhibited because neither can be preferred over the other. Conceivably both qualifying protons could transfer, but this yields the same ionic species as before. In either case (zero or two protons transferred) the fragments would rebound and again collide in a finite time since some of the initial kinetic energy would be converted to rotation and vibration at first encounter. Quite clearly there can be, with correspondingly lower probabilities, multiple rebound collisions in which neutral products are formed only at the third, fourth, fifth, ... successive collision. We have no reason to believe that projecting anomalous collisions
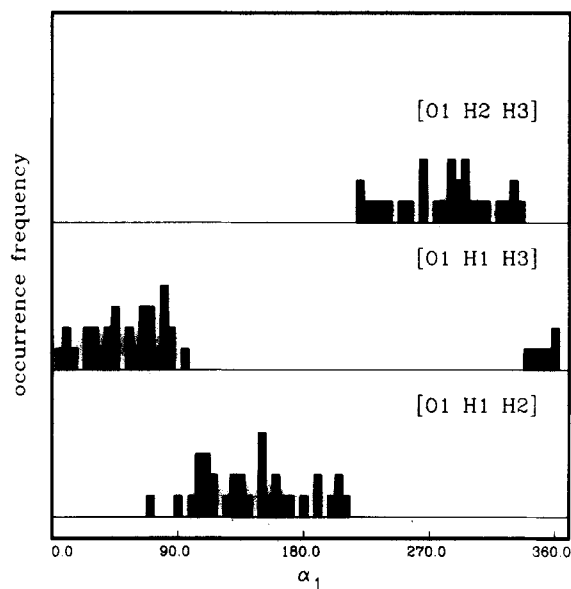

Figure 4. Identity of the transferred proton vs. the initial hydronium rotation angle α_1. The lowest histogram represents all cases in which H3 is transferred, the middle histogram those for H2, and the upper histogram those for H1. In all 99 cases H4 remained attached to O2 during the reaction.

out of the statistical analysis would seriously alter any of the calculated averages.

For each of the trajectories note was taken of which proton transferred from the hydronium to the hydroxide. An interesting pattern emerges when the results are presented in histogram form, Figure 4, vs. Euler angle α_1. This is the first angle of rotation applied to the hydronium, about its threefold axis, and effectively controls which of the hydrogens (H1, H2, H3) points preferentially toward the hydroxide. Although some slight overlap occurs, the result is essentially a set of three equivalent distributions, each spanning 120° along the α_1 axis. The separation between these populations is not complete because some reactant rotation can occur on the way in to collision from the initial 20 Å separation. Significantly, $\alpha_1 = 209.9°$ for the anomalous trajectory no. 47, close to the boundary between two of the distributions, thereby confirming the interpretation given above. Analogous plots for the other five Euler angles fail to yield similarly separated distributions.

The mean kinetic energy for center of mass motion of the product molecules was found to be 70.199 kcal/mol for the 99 collisions, with a root-mean-square deviation from the mean of 11.719 kcal/mol. Although this must be equally distributed between the two water molecules, the same is not necessarily the case for energy of internal motions. The mean *total* kinetic energy and its root-mean-square deviation are 77.563 and 14.635 kcal/mol, respectively, for that water molecule containing O1 (originally in the hydronium cation). By contrast the mean and deviation for the O2 water molecule (originally from the hydroxide anion) are 108.417 and 6.965 kcal/mol, respectively.

Figure 5 presents frequency plots of the fractions of mean kinetic energy, for the two distinguishable water molecules that are associated with internal motions, i.e.

$$[(K.E.)_{tot} - (K.E.)_{cm}]/(K.E.)_{tot} \qquad (8)$$

The results are dramatically different depending on the source of the water molecule. For the molecule incorporating O1 relatively little energy usually shows up in the internal motions, though infrequent exceptions occur. On
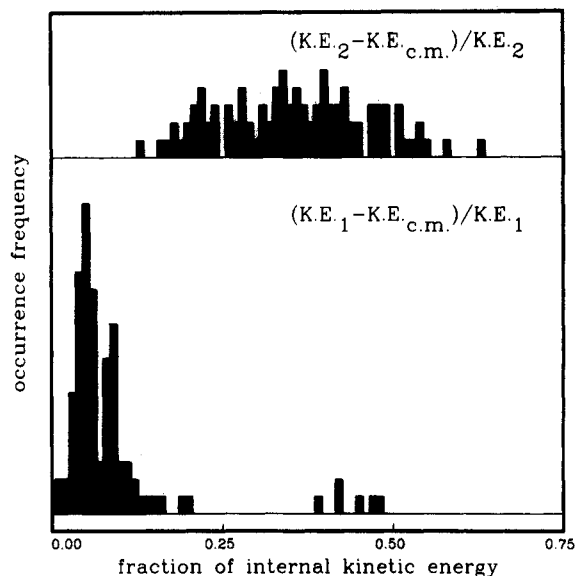
Figure 5. Distributions of the time-averaged kinetic energies attributable to internal modes of product molecules. The upper distribution refers to the molecule containing the hydroxide oxygen 02, the lower distribution to the molecule containing the hydronium oxygen 01.

the other hand, the O2 water molecule tends to be internally much "hotter." In 88 out of 99 collisions the final kinetic energy of the O2 product molecule exceeded that of the O1 product molecule by *more* than the characteristic ratio 19/17 that described the incident kinetic energies of the corresponding reactant clusters.

It seems obvious that the inequivalence of the distributions in Figure 5 has its source in the unidirectionality of the proton transfer. Just at the instant that the transferring proton is midway between the two oxygens, it forms a severely stretched OH bond. This stretching constitutes a high degree of vibrational excitation for the acceptor molecule which carries that proton away, no analogue of which exists for the donor molecule. As the donated proton falls inward to the hydroxide it can also confer rotational excitation.

Those few cases with high internal excitation (Figure 5, lower distribution) in the O1 molecule are found to be associated with atypically high total kinetic energy for this molecule.

IV. Conclusions

Our principal conclusion is that the polarization model offers a convenient tool for the study of gas-phase neutralization reactions. At least for the small clusters involved it is possible without inordinate expense to generate a relatively large number of trajectories, each over a sufficiently large time interval, so that product distribution functions can be determined with reasonable reliability. As reactant cluster size increases it becomes more expensive to construct numerical trajectories, and the number of product channels tends to increase.[8] Nevertheless, our experience suggests that neutralization reactions could be studied readily for cases involving the stoichiometric equivalent of ten water molecules, e.g.

$$H_{11}O_5^+ + H_9O_5^- \rightarrow 10H_2O \qquad (9)$$
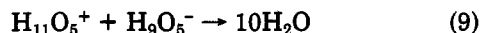
The important question of whether the polarization model can yield reliable and accurate predictions for these neutralization reactions will probably have to await the development of an experimental method which can produce data for comparison. We are aware that the simple initial conditions (zero initial reactant energy) used for the present calculations may not correspond to what will

prevail in such future experiments. However, those initial conditions are easily altered to simulate thermal populations or collimated beams. In the absence of experimental guidance it is premature to make an exhaustive computational study of the effects of initial conditions.

It is obvious that our calculations could easily be repeated with isotopic substitutions in the reactants. Labeling of this sort would be required experimentally in order to confirm the asymmetry shown by results in Figure 5. We expect the following variants of reaction 1

$$D_3O^+ + OH^- \rightarrow D_2O + HDO$$

$$H_3O^+ + OD^- \rightarrow H_2O + HDO \qquad (10)$$
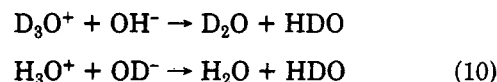
to continue to show the same basic energy disproportionation, though with some variation due to changed masses. However the products in (10) are now mass-distinguishable in a way which identifies their source.

The anomalous rebound trajectory illustrated in Figure 3 will have nonreactive analogues for higher incident energies. Instead of falling inward a second time to react, that higher energy would permit escape. The reason for lack of reaction is as before, namely near symmetry in the geometry of the collision complex leading to proton transfer ambiguity. Our calculations lead to the conclusion that a small proportion ($<10^{-2}$) of the collisions should be found to be nonreactive.

We hope that the calculations reported here will encourage experimentalists to undertake direct studies of these interesting gas-phase neutralization reactions.

Appendix

In the present version of the polarization model (denoted by PM6), the potential is composed of an atomic-pair and an induced-dipolar interaction. Using Å as the distance unit and kcal/mol as the energy unit, the first interaction has been specified by three pair potentials with the following forms

$$\phi_{HH}(r) = 332.1669/r$$

$$\phi_{OH}(r) = (332.1669/r)[13.59449911 \times$$
$$\exp(-4.050595693r) - 2] + 10 \exp(-3(r - 1.6)^2) -$$
$$198.0722802(r - r_e) \exp(-16(r - r_e)^2)$$

and

$$\phi_{OO}(r) = \frac{1328.6676}{r} + 24.779 \exp[-5.113(r - 2.45)] +$$
$$\frac{33.445}{1 + \exp[11.739(r - 2.49)]} + \frac{3.660}{1 + \exp[3.975(r - 3.77)]}$$

In the ϕ_{OH} interaction the value of r_e has been taken as 0.9854 Å, the equilibrium bond length of water. This particular parameterization of the polarization model is somewhat different from those previously used.[14]

The polarization interaction requires the self-consistent calculation of an induced dipole moment for each of the oxygen atoms. At each time step of the dynamical calculation, the following matrix equations must be solved[7]

$$A(r)\mu = X(r)$$

and

$$A(r)\nu = Y(r)$$

where μ is the induced dipole for each oxygen atom and ν is a Lagrange multiplier required for the calculation of the force.[7] The A matrix has elements

$$(A)_{lm} = 1 - \alpha \sum_{m(\neq l)} \frac{T_{lm}}{r_{lm}^3} [1 - K_0(r_{lm})]$$

where $\alpha = 1.444$ Å^3, the sum is over all other oxygen atoms and

$$\mathbf{T}_{lm} = 1 - 3\frac{\mathbf{r}_{lm}\mathbf{r}_{lm}}{r_{lm}^2}$$

The vector $\mathbf{X}(r)$ is given as

$$(\mathbf{X}(r))_l = \alpha \sum_{j(\neq l)} \frac{\mathbf{r}_{lj}}{r_{lj}^3} q_j [1 - K_O(r_{lj})]$$

while the vector $\mathbf{Y}(r)$ is given as

$$(\mathbf{Y}(r))_l = \alpha \sum_{j(\neq l)} \frac{\mathbf{r}_{ij}}{r_{ij}^3} q_j [1 - L_O(r_{ij})]$$

where the sums are over all other charges. The polarization energy associated with the induced moments is given as

$$\Phi_{\text{pol}} = \frac{1}{2} \sum_{j \neq l} \frac{(\mu_l \mathbf{r}_{lj}) q_j}{r_{lj}^3} [1 - L_O(r_{lj})]$$

The dimensionless factors $1 - K_O$ and $1 - L_O$ account for the spatial extension of the polarizable electron cloud about each oxygen. In the current parameterization the functions have been specified as

$$1 - K_O(r) = r^3/[r^3 + k(r)]$$

where

$$k(r) = 2.116045232(r - r_e)^2 \exp[-8(r - r_e)^2] + 20.33584298 \exp(-2.8924958r)$$

and

$$1 - L_O(r) = 1 - 0.5[L_1(r) + L_2(r)]$$

with

$$L_1(r) = [0.30/(r^3 + 0.30)] + 0.4189697616r^3 \times \exp[-5.685253959(r - 0.9678133088)^2]$$

$$L_2(r) = \exp(-3.160792364r)[1 + 3.160792364r + 4.995304184r^2 - 24.59792968r^3 + 30.71934979r^4]$$